

The angular momentum of disc galaxies: implications for gas accretion, outflows, and dynamical friction

Aaron A. Dutton^{1*}†, Frank C. van den Bosch²

¹*Department of Physics and Astronomy, University of Victoria, Victoria, BC, V8P 5C2, Canada*

²*Astronomy Department, Yale University, P.O. Box 208101, New Haven, CT 06520-8101, USA*

Accepted 2011 December 5. Received 2011 October 29; in original form 2011 June 2

ABSTRACT

We combine constraints on the galaxy-dark matter connection with structural and dynamical scaling relations to investigate the angular momentum content of disc galaxies. For haloes with masses in the interval $10^{11.3}M_{\odot} \lesssim M_{\text{vir}} \lesssim 10^{12.7}M_{\odot}$ we find that the galaxy spin parameters are basically independent of halo mass with $\langle \lambda'_{\text{gal}} \rangle \equiv (J_{\text{gal}}/M_{\text{gal}})/(\sqrt{2}R_{\text{vir}}V_{\text{vir}}) = 0.019_{-0.003}^{+0.004}$ (1σ). This is significantly lower than for relaxed Λ CDM haloes, which have an average spin parameter $\langle \lambda'_{\text{halo}} \rangle = 0.031 \pm 0.001$. The average ratio between the specific angular momentum of disc galaxies and their host dark matter haloes is therefore $\mathcal{R}_j \equiv \lambda'_{\text{gal}}/\lambda'_{\text{halo}} = 0.61_{-0.11}^{+0.13}$. This calls into question a standard assumption made in the majority of all (semi-analytical) models for (disc) galaxy formation, namely that $\mathcal{R}_j = 1$. Using simple disc formation models we show that it is particularly challenging to understand why \mathcal{R}_j is independent of halo mass, while the galaxy formation efficiency (ϵ_{GF} , proportional to the ratio of galaxy mass to halo mass) reveals a strong halo mass dependence. We argue that the empirical scaling relations between ϵ_{GF} , \mathcal{R}_j and halo mass require both feedback (i.e., galactic outflows) and angular momentum transfer from the baryons to the dark matter (i.e., dynamical friction). Most importantly, the efficiency of angular momentum loss need to decrease with increasing halo mass. Such a mass dependence may reflect a bias against forming stable discs in high mass, low spin haloes or a transition from cold-mode accretion in low mass haloes to hot-mode accretion at the massive end. However, current hydrodynamical simulations of galaxy formation, which should include these processes, seem unable to reproduce the empirical relation between ϵ_{GF} and \mathcal{R}_j . We conclude that the angular momentum build-up of galactic discs remains poorly understood.

Key words: galaxies: formation — galaxies: fundamental parameters — galaxies: spirals — galaxies: structure

1 INTRODUCTION

In the current paradigm of galaxy formation, galaxy discs are considered to form from the accretion of gas inside hierarchically growing cold dark matter (CDM) haloes (see Mo, van den Bosch & White 2010 for a comprehensive overview). The dark matter (DM) and gas acquire angular momentum via tidal torques in the early Universe (Peebles 1969). When gas accretes onto the central galaxy, this angular momentum may eventually halt the collapse and lead to the formation of a rotationally supported disc (Fall & Efstathiou 1980). If the specific angular momentum of the baryons is conserved during galaxy formation, there is enough angular momentum to

make galaxy discs with the observed sizes (e.g., Dalcanton et al. 1997; Mo, Mao, & White 1998; Firmani & Avila-Reese 2000; de Jong & Lacey 2000; Navarro & Steinmetz 2000). In fact, models in which galaxies have $\sim 30\%$ lower specific angular momentum than their dark matter haloes may be preferred (Dutton et al. 2007). Another success of this picture is that the large variation in the specific angular momentum of dark matter haloes, at fixed halo mass, explains the large scatter in disc sizes, or equivalently surface brightnesses, at fixed luminosity (Dalcanton et al. 1997). This picture also accounts for the time evolution of disc sizes (Somerville et al. 2008; Firmani & Avila-Reese 2009; Dutton et al. 2011a), reproducing the observed weak evolution since redshift $z \simeq 1$ (Barden et al. 2005), and the stronger

* dutton@uvic.ca

† CITA National Fellow

evolution observed from $z \sim 2$ to $z \sim 1$ (Trujillo et al. 2006; Williams et al. 2010).

Despite the many successes of these models, all of which assume that specific angular momentum is conserved during galaxy formation, there are several reasons, from a physical point of view, as to why the ratio between the specific angular momentum of the baryons and that of the dark matter halo, denoted \mathcal{R}_j ¹, might be different from unity:

(i) Selective accretion of baryons. If not all available baryons make it into the galaxy, the specific angular momentum of the galaxy can be either higher ($\mathcal{R}_j > 1$) or lower ($\mathcal{R}_j < 1$) than that of all baryons (whether it is higher or lower simply depends on the specific angular momentum distribution of the materials that *are* selected). An example of a selective accretion process is cooling. Cooling is generally an inside-out process, with the inner regions cooling prior to the more outer regions. Since the mass of Λ CDM haloes is more concentrated than the specific angular momentum (see e.g., Navarro & Steinmetz 1997), one expects that $\mathcal{R}_j < 1$ if not all baryons manage to cool.

(ii) Exchange of angular momentum between the dark matter and the baryons. An example of this is dynamical friction, which transfers orbital angular momentum from the baryons to the dark matter, thus resulting in $\mathcal{R}_j < 1$ (e.g., Navarro & Benz 1991; Navarro & White 1994). The strength of this process depends on the efficiency of star formation at early times. If the formation of baryonic clumps can be suppressed, such as through strong feedback, then the angular momentum transfer is reduced (e.g., Weil, Eke & Efstathiou 1998; Sommer-Larsen, Gelato & Vedel 1999; Eke, Efstathiou & Wright 2000).

(iii) Feedback. If feedback (from supernova, AGN or any other mechanism) results in the removal of gas, one can achieve values for \mathcal{R}_j that are very different from unity by simply removing a specific subset of the baryons. As an example, several studies have argued that supernova feedback affects low angular momentum material more than high angular momentum material, causing a net increase of \mathcal{R}_j (Maller & Dekel 2002; Dutton & van den Bosch 2009; Dutton 2009; Governato et al. 2010; Brook et al. 2011).

Cosmological hydrodynamical simulations almost invariably predict that disc galaxies have significantly less specific angular momentum than their dark matter haloes ($\mathcal{R}_j < 1$), suggesting that mechanisms (i) and (ii) discussed above play an important role. Early simulations in a standard cold dark matter (SCDM) cosmology (i.e. $\Omega_m = 1, \Omega_\Lambda = 0$) resulted in a catastrophic loss of angular momentum (Navarro & Benz 1991; Navarro & White 1994; Steinmetz & Navarro 1999), producing discs an order of magnitude too small. More recent simulations in Λ Cold Dark Matter (Λ CDM) cosmologies have resulted in less angular momentum loss, but typical ratios between the specific angular momentum of the baryons and that of the dark matter are $\mathcal{R}_j \simeq 50\%$ (Piontek & Steinmetz 2011; Sales et al. 2010). This “angular momentum loss” is sometimes

attributed to lack of numerical resolution (e.g. Governato et al. 2004; Kaufmann et al. 2007). However, Piontek & Steinmetz (2009) argue that the dominant cause is dynamical friction between clumps of baryons and the dark matter halo. If, based on these findings, we assume that angular momentum loss is a natural feature of disc galaxy formation in a Λ CDM universe, a relevant question is the following: *If the baryons that make up a discy galaxy carry half the specific angular momentum of the dark matter halo in which they reside, is it possible to reproduce in detail the observed sizes of disc galaxies?*

This question was addressed by Navarro & Steinmetz (2000). Using scaling relations between disc size, luminosity, and rotation velocity, these authors derived an expression for \mathcal{R}_j (f_j in their notation) that depends on the galaxy formation efficiency, $\epsilon_{\text{GF}} \equiv (M_{\text{gal}}/M_{\text{vir}})/(\Omega_b/\Omega_m)$ (f_{bdsk} in their notation), cosmic matter density, Ω_m , and stellar mass-to-light ratio, Υ_I . They found that if the rotation speeds of galaxy discs are approximately the same as the circular velocities of their surrounding haloes (which has subsequently been shown to be the case, at least on average, by Dutton et al. 2010b), then discs must have retained about half of the available specific angular momentum during their assembly. Another result from this analysis is that disc galaxies forming in low density cosmologies, such as Λ CDM, need to have $\mathcal{R}_j \simeq 2 \epsilon_{\text{GF}}$, that is, they draw a larger fraction of the specific angular momentum than the galaxy formation efficiency. This is at odds with the expectation (see § 4.1 below) that $\mathcal{R}_j \simeq \epsilon_{\text{GF}}$ if the galaxy formation efficiency is mainly determined by the inefficiency of cooling.

Thus observational measurements of the specific angular momentum in galaxies place constraints on the way galaxies acquire their mass and angular momentum. The specific angular momentum of the dark matter, $J_{\text{vir}}/M_{\text{vir}}$, where J_{vir} is the total angular momentum, and M_{vir} is the total virial mass, is commonly expressed in terms of the dimensionless spin parameter (Peebles 1969):

$$\lambda_{\text{halo}} = \frac{J_{\text{vir}}|E|^{1/2}}{GM_{\text{vir}}^{5/3}} = \frac{J_{\text{vir}}/M_{\text{vir}}}{\sqrt{2}R_{\text{vir}}V_{\text{vir}}} f_c^{1/2} = \lambda'_{\text{halo}} f_c^{1/2} \quad (1)$$

Here E is the halo’s energy, R_{vir} is the virial radius, V_{vir} is the circular velocity at the virial radius, and f_c measures the deviation of E from that of a singular isothermal sphere truncated at R_{vir} . It is common to set $f_c = 1$ (Bullock et al. 2001), so that the spin parameter only depends on the total angular momentum and mass of the halo. In this case the spin parameter is denoted λ'_{halo} . The equivalent spin parameter for the galaxy is defined as

$$\lambda'_{\text{gal}} = \frac{(J_{\text{gal}}/M_{\text{gal}})}{\sqrt{2}R_{\text{vir}}V_{\text{vir}}}, \quad (2)$$

(see Section 2.1 for details).

Dark matter only cosmological simulations have shown that both λ_{halo} and λ'_{halo} are log-normally distributed (e.g., Bullock et al. 2001) with median and scatter independent of halo mass (e.g., Macciò et al. 2007; Bett et al. 2007; Muñoz-Cuartas et al. 2011) and independent of environment (Lemson & Kauffmann 1999, Macciò et al. 2007). For relaxed haloes identified with a spherical overdensity (SO) algorithm Macciò et al. (2008) find a median value of $\lambda'_{\text{halo}} = 0.031 \pm 0.001$. Using a similar halo definition Bett et al. (2007) find a median $\lambda_{\text{halo}} = 0.0367$. For the cosmol-

¹ Note that in the notation of Mo, Mao, & White (1998), $\mathcal{R}_j = (j_d/m_d)$, where j_d is the ratio between the *angular momentum* of the disc and dark matter halo, and m_d is the ratio between the *mass* of the disc and dark matter halo.

ogy adopted by Bett et al. , $f_c \simeq 1.3$ for a $10^{12} M_\odot$ halo, and thus $\lambda'_{\text{halo}} \simeq 0.032$, which is in excellent agreement with the results of Macciò et al. (2008). Simulations with gas in which there is no cooling find similar spin parameters for the baryons and dark matter (van den Bosch et al. 2002; Sharma & Steinmetz 2005). Thus in what follows we assume that the median spin parameter of the halo is

$$\lambda'_{\text{halo}} = 0.031 \pm 0.001. \quad (3)$$

The main goal of this paper is to determine the average value of \mathcal{R}_j for a large sample of disc galaxies as a function of their halo mass, and to use semi-analytical models to explore implications for how disc galaxies form. Since it is impossible to measure the specific angular momentum (or spin parameter) of a real (as opposed to simulated) dark matter halo, one can only obtain an estimate for the *average* value of \mathcal{R}_j by comparing the *distribution* of galaxy spin parameters, λ'_{gal} , obtained from a sample of galaxies to the *distribution* of halo spin parameters, λ'_{halo} , obtained from numerical simulations of structure formation in a Λ CDM cosmology. This is the approach we will follow in this paper.

Measuring λ'_{gal} for an individual galaxy necessarily involves the following steps:

- (i) Determine the specific angular momentum of the baryons.
- (ii) Determine the mass (and virial radius) of the dark matter halo in which the galaxy resides.

Step (i) is relatively straightforward. Using that, for a disc galaxy,

$$J_{\text{gal}} = 2\pi \int_0^{R_{\text{vir}}} \Sigma(R) V_{\text{rot}}(R) R dR, \quad (4)$$

it is clear that one can determine the angular momentum of a disc galaxy from measurements of its surface mass density, $\Sigma(R)$, (accounting for both gas and stars), and its rotation curve $V_{\text{rot}}(R)$ (see e.g., van den Bosch, Burkert & Swaters 2001). Alternatively, since disc galaxies in general have exponential surface density profiles and flat rotation curves, one can use simple scaling relations between mass (or luminosity), size and characteristic rotation velocity in order to obtain an estimate of J_{gal} without having to measure $\Sigma(R)$ or $V_{\text{rot}}(R)$ (e.g., Navarro & Steinmetz 2000; Tonini et al. 2006; Hernandez & Cervantes-Sodi 2006; Hernandez et al. 2007; Berta et al. 2008). Although less accurate than using Eq. (4), this method has the advantage that it can be applied to much larger samples of galaxies. Step (ii) is a little bit more involved. Typically, accurate measurements of halo mass require probes on scales of the virial radius. Examples of such ‘probes’ are gravitational lensing, X-ray data and satellite kinematics. However, unless the galaxy in question is the central galaxy of a cluster-sized halo, such measurements are rarely available for individual systems, and one has to rely on uncertain estimates of the halo mass from the galaxy’s rotation curve. Alternatively, one can use various statistical techniques to assign to each galaxy an *average* halo mass. Recent years have seen dramatic progress in using a variety of techniques to constrain the average relation between galaxy properties (typically luminosity of stellar mass) and halo mass, in particular from galaxy clustering (e.g., Yang, Mo & van den Bosch 2003; Tinker et al. 2005),

galaxy-galaxy lensing (e.g. Mandelbaum et al. 2006; Cacciato et al. 2009), abundance matching (e.g., Conroy, Wechsler & Kravtsov 2006), and satellite kinematics (e.g., More et al. 2009).

In this paper we compute the average specific angular momentum and spin parameters of disc galaxies as a function of their halo mass. We improve on previous studies in a number of ways. We constrain halo masses using recent results for the halo mass - stellar mass relation for disc galaxies obtained from weak gravitational lensing and satellite kinematics (Dutton et al. 2010b), rather than abundance matching results as in Tonini et al. (2006), or the highly questionable assumption of a constant galaxy mass fraction made by Hernandez & Cervantes-Sodi (2006), Hernandez et al. (2007), and Berta et al. (2008). We also improve upon these studies by taking account of realistic uncertainties on halo masses. We consider both stellar and gaseous discs, rather than just stellar discs, which is important for low mass galaxies which tend to be gas rich (Tonini et al. 2006). We calculate disc angular momentum by integrating a model that is constructed to reproduce the size-mass and velocity-mass (i.e., Tully-Fisher, Tully & Fisher 1977) relations, rather than simple scaling arguments for exponential discs in isothermal haloes (i.e., $J_{\text{gal}}/M_{\text{gal}} = 2R_d V_{\text{rot}}$), as used by e.g., Navarro & Steinmetz (2000) and Hernandez et al. (2007). We also discuss how uncertainties related to stellar mass-to-light ratios and adiabatic contraction impact the inferred values of \mathcal{R}_j , and use simple models of disc galaxy formation to discuss the implications of our findings for cooling, outflows and angular momentum loss.

We adopt a flat Λ CDM cosmology with matter density parameter $\Omega_m = 0.27$, baryon density $\Omega_b = 0.044$, and Hubble parameter $h = H_0/100 \text{ km s}^{-1} \text{ Mpc}^{-1} = 0.7$. Dark matter halo masses are defined so that the mean density of the halo (assumed to be spherical) is 200 times the critical density.

2 DEFINITIONS AND MASS MODELS

This section gives a brief overview of the main parameters we discuss in this paper, and the constrained mass models we use to constrain them.

2.1 Mass and Angular Momentum Parameters

There are four main parameters that are relevant for what follows: galaxy mass, M_{gal} , halo virial mass, M_{vir} , galaxy angular momentum, J_{gal} , and the angular momentum of the dark matter halo, J_{vir} . The galaxy mass is the sum of the mass in stars and cold gas. The virial mass is the total mass (stars, cold gas, hot gas, dark matter) within the virial radius. The galaxy angular momentum is the sum of the angular momenta of the stars and of the cold gas. The virial angular momentum is the total angular momentum within the virial radius.

Our main goal is to constrain the angular momentum ratio, \mathcal{R}_j , defined as the ratio between the galaxy specific

angular momentum and the total specific angular momentum²:

$$\mathcal{R}_j \equiv \frac{(J_{\text{gal}}/M_{\text{gal}})}{(J_{\text{vir}}/M_{\text{vir}})} = \frac{\lambda'_{\text{gal}}}{\lambda'_{\text{halo}}}, \quad (5)$$

where the spin parameters λ'_{halo} and λ'_{gal} are defined by Eqs. (1) and (2), respectively. Using that for disc galaxies $J_{\text{gal}} \propto R_{\text{d}} M_{\text{gal}} V_{\text{rot}}$, where R_{d} is the disc scale length and V_{rot} is a characteristic rotation velocity of the disc, one can use Eq. (5) to show that

$$R_{\text{d}} \propto \mathcal{R}_j \lambda'_{\text{halo}} \left(\frac{V_{\text{rot}}}{V_{\text{vir}}} \right)^{-1} R_{\text{vir}}, \quad (6)$$

which is the standard approach used in analytical and semi-analytical models to predict the sizes of disc galaxies (e.g., Kauffmann 1996; Mo, Mao & White 1998; Somerville & Primack 1999; van den Bosch 2000; Cole et al. 2000). In many cases these studies simplify Eq. (5) by assuming that $\mathcal{R}_j = 1$ and that $V_{\text{rot}}/V_{\text{vir}}$ is a constant. In this paper we examine whether there is empirical support for the former assumption and what this implies for the formation of disc galaxies in general. As we will demonstrate, it is instructive to compare \mathcal{R}_j to the galaxy formation efficiency parameter

$$\epsilon_{\text{GF}} \equiv \frac{(M_{\text{gal}}/M_{\text{vir}})}{(\Omega_{\text{b}}/\Omega_{\text{m}})}. \quad (7)$$

which describes what fraction of the cosmologically available baryons have ended up in a galaxy.

2.2 Mass Models

We compute the *average* value for \mathcal{R}_j for disc galaxies using the mass models of Dutton et al. (2011b), which have been constructed to reproduce the observed structural and dynamical scaling relations of late-type (i.e., star-forming and disc-dominated) galaxies. They consist of four components: a stellar bulge, a stellar disc, a gas disc, and a dark matter halo. Both the bulge and the dark matter halo are assumed to be spherical and to follow a density distribution that is given by a Hernquist profile (Hernquist 1990) and a NFW profile (Navarro, Frenk, & White 1997), respectively. The density profile of the halo, however, is modified to account for the gravitational response to galaxy formation (most often modelled as adiabatic contraction, see Blumenthal et al. 1986). The disc is assumed to have an exponential surface density and to be infinitesimally thin.

Each halo-galaxy system is described by nine parameters: three for the halo (virial mass, M_{vir} , concentration, c , and a parameter that describes the impact of galaxy formation on the halo density profile); and six for the baryons (stellar mass, M_{star} , gas mass, M_{gas} , bulge fraction, f_{b} , bulge size, R_{b} , stellar disc size, R_{d} , and gas disc size, R_{g}). The 6 parameters for the baryons are constrained by the observed scaling relations: R_{b} vs. M_{star} ; R_{d} vs. M_{star} ; $R_{\text{g}}/R_{\text{d}}$ vs. M_{star} ; f_{b} vs. M_{star} , and $M_{\text{gas}}/M_{\text{star}}$ vs. M_{star} (see Dutton et al. 2011b for details). For the relation between M_{vir} and M_{star} we use the empirical relation from Dutton et al. (2010b), which is inferred from a large number of independent studies and techniques, including galaxy-galaxy

lensing, satellite kinematics, galaxy clustering, and abundance matching. We will use the scatter among these different studies/techniques, as an estimate for the uncertainty in the M_{vir} vs. M_{star} relation, and propagate these uncertainties to those on ϵ_{GF} and \mathcal{R}_j . Finally, the relation between halo mass, M_{vir} , and halo concentration, c , is taken from Macciò et al. (2008), and is calibrated using high-resolution numerical simulations.

The usage of all these empirical and theoretical scaling relations implies that the nine model parameters can be reduced to two primary unknowns: the stellar initial mass function (IMF), and a prescription for how galaxy growth influences the structural properties of the dark matter halo (hereafter “the halo contraction model”). It is common practice to assume that disc formation is an adiabatic process and that the halo responds by contracting using the adiabatic contraction (hereafter AC) prescription of Blumenthal et al. (1986; hereafter BFFP). However, numerical simulations have shown that this prescription may not be sufficiently accurate, and several alternatives have been proposed (e.g., Gnedin et al. 2004; Abadi et al. 2010). We follow Dutton et al. (2007) and use a generalized halo contraction model, according to which a shell of dark matter initially (before disc formation) at radius r_i ends up, after disc formation, at a radius

$$r_f = \Gamma_{\text{BFFP}}^{\nu} r_i. \quad (8)$$

Here Γ_{BFFP} is the amount of contraction as predicted by the AC-model of BFFP, and ν is a free parameter. Note that $\nu = 1$ corresponds to the standard adiabatic contraction model of BFFP, while the Gnedin et al. (2004) and Abadi et al. (2010) models can be well approximated by $\nu = 0.8$ and $\nu = 0.4$, respectively. A model without contraction has $\nu = 0$, while $\nu < 0$ indicates that the dark matter halo responds to disc formation by expanding.

As shown in Dutton et al. (2011b), reproducing the observed Tully-Fisher relation implies different values for ν for a different choice of the IMF. In this paper we will consider two different models that fit the Tully-Fisher relation (and all other scaling relations mentioned above) equally well: model A which adopts a Chabrier (2003) IMF and $\nu = -0.5$ (i.e., halo expansion), and model B, in which we adopt the AC model of Gnedin et al. (2004), i.e., we set $\nu = 0.8$, and we assume an IMF that yields stellar mass-to-light ratios that are 0.3 dex lower than for the Chabrier (2003) IMF. As shown in Dutton et al. (2011b) both these models are in excellent agreement with the data. As we will show below, model B results in galaxy spin parameters that are ~ 30 percent (~ 0.12 dex) higher than those of model A. This uncertainty is comparable to that arising from the uncertainty in the M_{vir} vs. M_{star} relation. Throughout we will mainly present the results for model A, while occasionally showing, for comparison, the results for model B.

For a given choice of IMF and ν , the model completely specifies the mass distributions of disc-plus-bulge galaxies as a function of halo mass. From these mass models we compute the angular momentum of the baryons by evaluating Eq. 4, where the surface density is the sum of the surface densities of the gas and stars: $\Sigma(R) = \Sigma_{\text{gas}}(R) + \Sigma_{\text{star}}(R)$. We assume that the bulge has no net angular momentum. If we assumed that bulges follow the same rotation curve as the disc, then this would increase the specific angular mo-

² Note that \mathcal{R}_j is not an efficiency because it can be larger than unity.

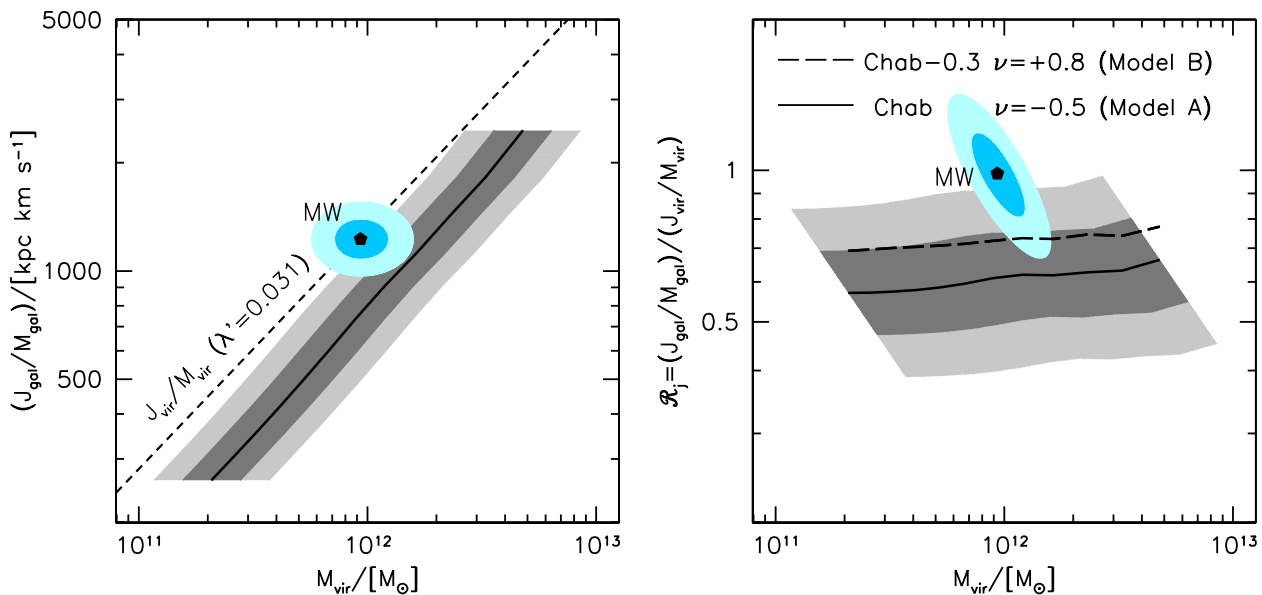


Figure 1. *Left:* Galaxy specific angular momentum vs. virial mass for disc galaxies. The shaded regions indicate the one and two σ uncertainties on virial mass. The dashed line shows the relation between virial specific angular momentum and virial mass from cosmological N-body simulations, corresponding to a spin parameter $\lambda' = 0.031$. The pentagon shows estimates for the Milky Way (MW) with the shaded region showing one and two σ uncertainties. *Right:* Specific angular momentum ratio (\mathcal{R}_j) vs. virial mass. The solid line and shaded regions indicate the mean and the one and two σ uncertainties for our fiducial model A, which assumes a Chabrier (2003) IMF and a halo contraction model characterized by $\nu = -0.5$. The dashed line shows the mean for model B, in which the stellar mass-to-light ratios are 0.3 dex smaller and $\nu = 0.8$. Note that, for both models, \mathcal{R}_j is less than unity and approximately independent of virial mass.

mentum of the galaxy by $\lesssim 20\%$. The effect is largest for the most massive galaxies, but since massive bulges, in general, are not rotationally supported, we believe our assumption that bulges have no angular momentum to be of no major concern for what follows.

As shown by Tonini et al. (2006) a significant fraction of the angular momentum of a galaxy is in the cold gas. In our models the cold gas in high mass galaxies ($M_{\text{gal}} \simeq 10^{11} M_{\odot}$) contains $\simeq 30\%$ of the angular momentum. This fraction rises to over 50% for galaxy masses below $M_{\text{gal}} \simeq 10^{10} M_{\odot}$. Thus if cold gas fractions increase at higher redshifts, as is commonly thought (but see Dutton et al. 2010a), measuring angular momentum of high redshift galaxies will require measurements of the distribution of cold gas, and not just the stars.

3 RESULTS

Using our constrained mass models we now discuss a number of correlations between mass and angular momentum of disc galaxies and dark matter haloes, and compare with previous results. These correlations are presented in Figs. 1-3 and Table 1.

3.1 Galaxy Mass and Specific Angular Momentum

The left-hand panel of Fig. 1 shows the correlation between galaxy specific angular momentum and virial mass for model A. The shaded regions show the one and two σ

uncertainties in virial masses at fixed galaxy mass³, which is the dominant source of uncertainty. The dashed line shows the relation between virial specific angular momentum and virial mass from cosmological N-body simulations (Macciò et al. 2008), which corresponds to a spin parameter of $\lambda' = 0.031$. The galaxy specific angular momentum scales with virial mass as $J_{\text{gal}}/M_{\text{gal}} \propto M_{\text{vir}}^{0.70}$, which is very similar to the virial scaling of $J_{\text{vir}}/M_{\text{vir}} \propto M_{\text{vir}}^{0.67}$. Thus the ratio \mathcal{R}_j between the galaxy and virial specific angular momentum is roughly constant (right-hand panel of Fig. 1). However, the galaxy specific angular momentum is significantly lower than the virial specific angular momentum with $\mathcal{R}_j = 0.61^{+0.13}_{-0.11}$ (1σ) for a virial mass of $M_{\text{vir}} = 10^{12} M_{\odot}$. The dashed line in the right-hand panel of Fig. 1 corresponds to model B, and is shown for comparison. Note that the combination of halo contraction and lower stellar mass-to-light ratios result in \mathcal{R}_j values that are ~ 0.1 higher than for our fiducial model A. This difference is comparable to the 1σ uncertainty on \mathcal{R}_j due to the uncertainties in the relation between stellar mass and halo mass.

The left-hand panel of Fig. 2 shows the correlation between galaxy mass and virial mass for the disc galaxies considered here. The dashed line shows the relation for the cosmically available baryonic mass, i.e., $M_{\text{gal}} = (\Omega_b/\Omega_m)M_{\text{vir}}$, corresponding to $\epsilon_{\text{GF}} = 1$. The right-hand panel of Fig. 2 shows the galaxy formation efficiency, ϵ_{GF} , which is the ratio between the solid and dashed lines in the left-hand

³ Note that these are the uncertainties on the mean; they do not reflect the scatter.

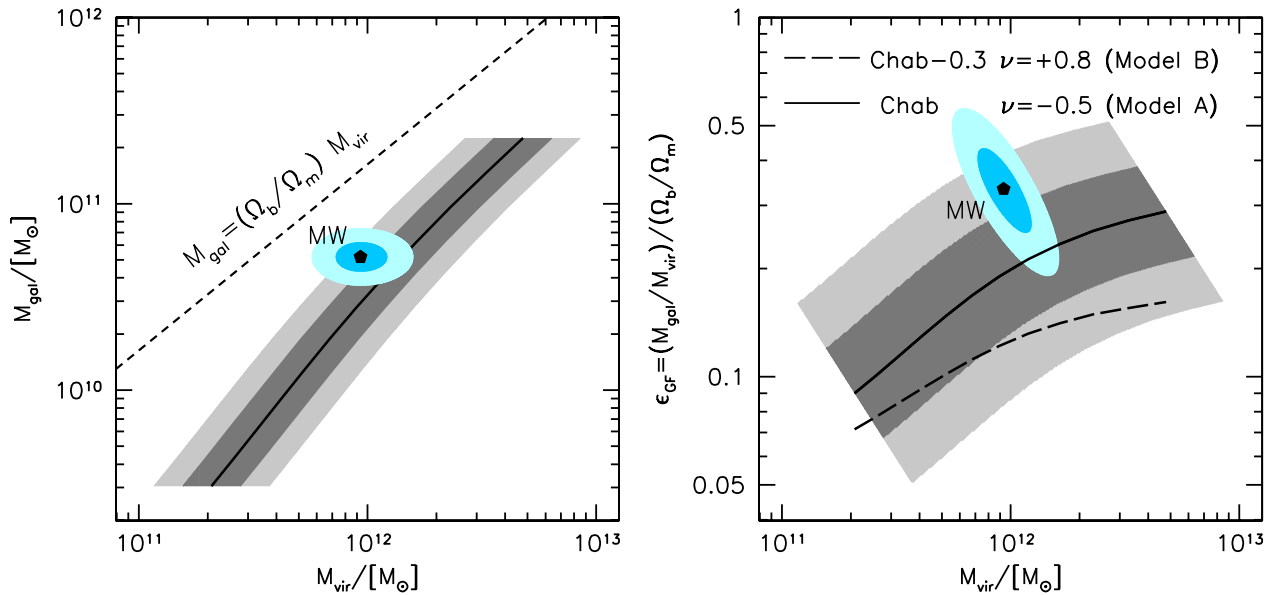


Figure 2. *Left:* Galaxy mass vs. virial mass for disc galaxies. The shaded regions reflect the one and two σ uncertainties on virial masses. The dashed line corresponds to the universal baryon fraction ($\Omega_b/\Omega_m = 0.163$). The pentagon shows estimates for the Milky Way (MW), with the shaded region showing one and two σ uncertainties. *Right:* Galaxy formation efficiency (ϵ_{GF}) vs. virial mass. As in Fig. 1, we show the results for both models A and B. For clarity, we only show the impact of virial mass uncertainties for our fiducial model A. Note that unlike \mathcal{R}_j , which reveals no significant dependence on halo mass (see Fig. 1), the galaxy formation efficiency varies by a factor of ~ 3 over the mass range probed.

panel. Unlike the angular momentum ratio, the galaxy formation efficiency is a strong function of virial mass, varying by a factor of ~ 3 from $\epsilon_{\text{GF}} \simeq 0.1$ at the low mass end ($M_{\text{vir}} \sim 2 \times 10^{11} M_{\odot}$) to $\epsilon_{\text{GF}} \simeq 0.3$ at the high mass end ($M_{\text{vir}} \sim 5 \times 10^{12} M_{\odot}$). Once again, the dashed line in the right-hand panel corresponds to model B, which yields lower galaxy formation efficiencies due to the lighter IMF.

As we demonstrate and discuss below, (semi)-analytical models and hydrodynamical simulations of galaxy formation do generally not predict values of \mathcal{R}_j that are independent of halo mass, and if they do, the corresponding values of ϵ_{GF} are inconsistent with the empirical results inferred here.

3.2 Galaxy Spin Parameter

We now discuss the galaxy spin parameter, as this is a quantity that has been measured and interpreted by previous studies. Fig. 3 shows the average galaxy spin parameter as a function of halo virial mass. This is the same as the right-hand panel of Fig. 1, but with a zero point shift. As discussed above, there is a slight mass dependence to λ'_{gal} , but given the uncertainties in halo masses, λ'_{gal} is consistent with being independent of halo mass. The normalization is $\simeq 60\%$ lower than predicted for Λ CDM haloes (dashed line). There are two simple interpretations of this result. One is that the baryons that form disc galaxies have lost about 40% of their angular momentum during galaxy formation, which could occur via dynamical friction. Another is that the baryons that form disc galaxies have 40% lower specific angular momentum than the cosmically available baryons, which could occur due to feedback and/or inefficient cooling. We discuss these interpretations in more detail in § 4.

An interpretation advocated by Tonini et al. (2006) is that if one restricts attention to haloes that have not experienced a major merger since $z \sim 3$, the average spin parameter λ' turns out to be around 0.023 (D'Onghia & Burkert 2004). This is motivated by the idea that bulge-less disc galaxies require a quiescent merger history. However, this simple expectation has been cast into doubt by numerical simulations which have shown that (gas rich) discs can survive major mergers (e.g., Springel & Hernquist 2005; Hopkins et al. 2009). While we cannot rule out a merger history bias for massive disc galaxies, we argue that such a bias cannot occur for low mass galaxies ($M_{\text{gal}} \lesssim 3 \times 10^{10} M_{\odot}$, $M_{\text{vir}} \lesssim 10^{12} M_{\odot}$) because typical low mass galaxies are bulge-less, and thus must form in haloes with typical merger histories (and hence typical halo spins).

3.3 Comparison with the Milky Way

As a reference, the black pentagons and light blue shaded regions in Figs. 1 & 2 show estimates for the specific angular momentum and mass of the Milky Way (MW). Here we have estimated the specific angular momentum of the MW assuming $J_{\text{gal}}/M_{\text{gal}} = 2R_d V_{\text{rot}}$, which is appropriate for an exponential disc with a flat rotation curve. We adopt $R_d = 2.8 \pm 0.23 \text{ kpc}(1\sigma)$ based on the dynamical models of Widrow et al. (2008) and $V_{\text{rot}} = 219 \pm 20 \text{ km s}^{-1}(1\sigma)$ from the observations of Reid et al. (1999). For the baryonic mass of the MW we use the bulge and disc masses, again from the dynamical models of Widrow et al. (2008) to obtain $\log_{10}(M_{\text{gal}}/M_{\odot}) = 10.71 \pm 0.075 (1\sigma)$. For the virial mass of the MW we average the results of Smith et al. (2007) and

Table 1. Relations between mass and angular momentum of galaxies and dark matter haloes for model A, as presented in Figs. 1-3. Uncertainties on halo masses are 1 and 2σ , and are propagated to other parameters as appropriate.

$\log_{10}(M_{\text{gal}})$ [M_{\odot}]	$\log_{10}(M_{\text{vir}})$ [M_{\odot}]	ϵ_{GF}	$\log_{10}(J_{\text{gal}}/M_{\text{gal}})$ [kpc km s $^{-1}$]	\mathcal{R}_j	λ'_{gal}
9.484	$11.318^{+0.125}_{-0.125} +0.250 -0.250$	0.09	$-0.03 -0.07$ $+0.02 +0.04$	2.417	$0.57 -0.10 -0.18$ $+0.12 +0.27$
9.631	$11.414^{+0.125}_{-0.125} +0.250 -0.250$	0.10	$-0.03 -0.08$ $+0.03 +0.04$	2.482	$0.57 -0.10 -0.18$ $+0.12 +0.27$
9.784	$11.513^{+0.125}_{-0.125} +0.250 -0.250$	0.11	$-0.04 -0.09$ $+0.03 +0.05$	2.550	$0.57 -0.10 -0.18$ $+0.12 +0.27$
9.941	$11.615^{+0.125}_{-0.125} +0.250 -0.250$	0.13	$-0.04 -0.10$ $+0.03 +0.06$	2.621	$0.58 -0.10 -0.19$ $+0.12 +0.27$
10.103	$11.720^{+0.125}_{-0.125} +0.250 -0.250$	0.15	$-0.06 -0.13$ $+0.04 +0.06$	2.697	$0.59 -0.10 -0.19$ $+0.12 +0.27$
10.270	$11.832^{+0.125}_{-0.125} +0.250 -0.250$	0.17	$-0.06 -0.15$ $+0.04 +0.07$	2.779	$0.60 -0.11 -0.19$ $+0.13 +0.28$
10.442	$11.950^{+0.125}_{-0.125} +0.250 -0.250$	0.19	$-0.07 -0.17$ $+0.05 +0.08$	2.868	$0.61 -0.11 -0.20$ $+0.13 +0.29$
10.618	$12.078^{+0.125}_{-0.125} +0.250 -0.250$	0.21	$-0.08 -0.18$ $+0.05 +0.09$	2.960	$0.62 -0.11 -0.20$ $+0.13 +0.29$
10.796	$12.215^{+0.125}_{-0.125} +0.250 -0.250$	0.23	$-0.08 -0.18$ $+0.06 +0.10$	3.050	$0.62 -0.11 -0.20$ $+0.13 +0.29$
10.979	$12.361^{+0.125}_{-0.125} +0.250 -0.250$	0.25	$-0.09 -0.21$ $+0.06 +0.11$	3.154	$0.63 -0.11 -0.20$ $+0.13 +0.29$
11.164	$12.517^{+0.125}_{-0.125} +0.250 -0.250$	0.27	$-0.10 -0.22$ $+0.07 +0.12$	3.261	$0.63 -0.11 -0.20$ $+0.13 +0.30$
11.352	$12.680^{+0.125}_{-0.125} +0.250 -0.250$	0.29	$-0.07 +0.13$ $+0.07 +0.13$	3.391	$0.66 -0.12 -0.21$ $+0.14 +0.31$

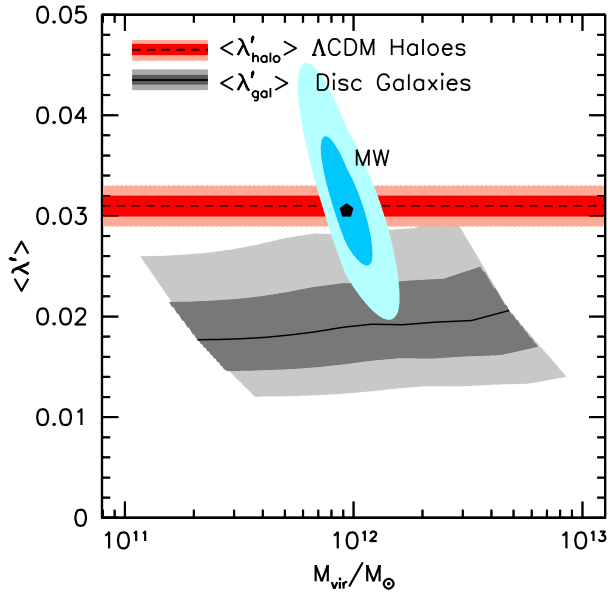


Figure 3. Average spin parameter *vs.* halo virial mass, for disc galaxies (solid line and grey shaded region), and Λ CDM dark matter haloes (dashed line, red shaded region). For the galaxy spin parameter the shaded regions show the one and two σ uncertainties introduced by the systematic uncertainty in halo masses. The pentagon shows an estimate for the Milky Way (MW) with the shaded region showing one and two σ uncertainties.

Xue et al. (2008) yielding $\log_{10}(M_{\text{vir}}/M_{\odot}) = 11.97 \pm 0.22$ (2σ).

The resulting galaxy spin parameter (see Eq.2) and galaxy formation efficiency (see Eq.7) of the MW are $\lambda'_{\text{gal}} = 0.031^{+0.016}_{-0.011}$ (2σ), and $\epsilon_{\text{GF}} = 0.033^{+0.28}_{-0.15}$ (2σ), respectively. Both λ'_{gal} and ϵ_{GF} are higher than for typical late-type galaxies. This could signify that the MW is atypical, or it could simply be a reflection of the measurement errors (especially in halo masses) both for the MW and for samples of late-type galaxies.

3.4 Comparison with Previous Studies

Several studies in the past used similar methods to determine the spin parameters of disc galaxies. These studies all find higher spin parameters than we find here, but as we show the differences can be ascribed to differences in the estimation of halo masses, which is the dominant source of systematic uncertainty in measuring the spin parameter.

Van den Bosch, Burkert & Swaters (2001; hereafter BBS01) used Eq. (4) and halo masses inferred from rotation curve modelling to determine the galaxy spin parameters for a sample of 14 disc-dominated dwarf galaxies. They found that $\langle \lambda'_{\text{gal}} \rangle = 0.048$ (see Fig. 4)⁴, albeit with a relatively large uncertainty due to the small sample size and the uncertainties in the stellar mass-to-light ratios and halo masses. At first sight, this is much larger than the average galaxy spin parameters inferred here; $\langle \lambda'_{\text{gal}} \rangle = 0.019$. However, there are several factors that can account for this large difference. BBS01 used dark halo masses and sizes derived from fits to rotation curves assuming adiabatic contraction. Since the rotation curves only extend to $\sim 10 - 20\%$ of the halo virial radius, this involves a significant extrapolation, and thus the potential for systematic errors. As discussed in detail in Dutton et al. (2007), the assumption that disc formation results in adiabatic contraction of its dark matter halo may not be realistic. The galaxies in BBS01 have a median $V_{\text{last}}/V_{\text{vir}} = 1.55$, where V_{last} is the rotation velocity at the last measured point (i.e., at the largest radius). Since dark matter haloes in the Λ CDM concordance cosmology have $V_{\text{max}}/V_{\text{vir}} \lesssim 1.2$, where V_{max} is the maximum circular velocity, the derived values from BBS01 are *strongly* influenced by the assumption of adiabatic contraction. Dutton et al. (2010b) have shown that the halo virial velocity is, on average, approximately equal to the optical rotation velocity. Using this assumption to derive halo masses results in $\log_{10}(M_{\text{vir}}/M_{\odot}) = 11.2 \pm 0.3$ and a median spin parameter $\lambda'_{\text{gal}} = 0.023$ (right-hand panel of Fig. 4). If we consider a 10% uncertainty on $V_{\text{rot}}/V_{\text{vir}}$ (Dutton et al. 2010b) then this

⁴ Here we have converted the results from BBS01 to the spin parameter definition of Bullock et al. (2001).

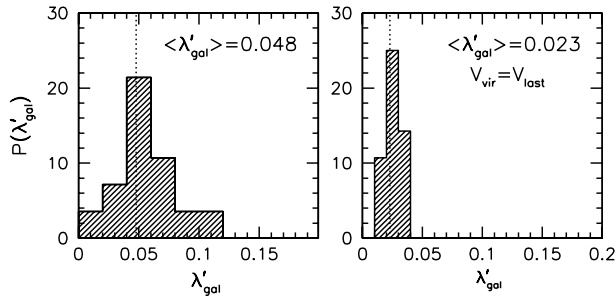


Figure 4. Histograms (hatched) of the distribution of galaxy spin parameters (λ'_{gal}) for the 14 disc dominated dwarf galaxies from van den Bosch, Burkert, & Swaters (2001; hereafter BBS01). In the left-hand panel λ'_{gal} has been obtained using the halo virial velocities from BBS01. In the right-hand panel, the halo virial velocities have been calculated assuming $V_{\text{vir}} = V_{\text{last}}$, where V_{last} is the rotation velocity at the last measured point (i.e., at the largest radius). The latter results in spin parameters in good agreement with our results (cf. Fig. 3).

results in a range of 0.019–0.028 for λ'_{gal} , which is consistent with our measured values (see Fig. 3).

Tonini et al. (2006) used average scaling relations between stellar mass, gas mass, halo mass and disc size to compute an average galaxy spin parameter as function of halo mass, under the assumption that dark matter haloes follow a Burkert (1995) profile. They found that $\langle \lambda'_{\text{gal}} \rangle \simeq 0.025 - 0.030$ with no significant dependence on halo mass. A comparison between the halo mass - stellar mass relation used by Tonini et al. (2006) and by ourselves indicates that their halo masses are a factor of ~ 2 lower than ours. This difference in halo masses fully accounts for their higher spin parameters.

Finally, Hernandez et al. (2007) determined the galaxy spin parameters for a large sample of galaxies taken from the Sloan Digital Sky Survey (SDSS). Rather than Tonini et al. (2006), they obtained estimates for λ_{gal} for *individual* galaxies using the method proposed by Hernandez & Cervantes-Sodi (2006), which is based on the following assumptions: (i) dark matter haloes are singular isothermal spheres, (ii) the self-gravity of the disc can be ignored, and (iii) all galaxies have the same ratio of dark matter mass to disc mass. In addition, they inferred the rotation velocity of each individual galaxy in a statistical sense, using an empirical Tully-Fisher relation. They found that for disc galaxies λ'_{gal} follows a log-normal distribution with $\langle \lambda'_{\text{gal}} \rangle \sim 0.059$, which is a factor of ~ 3 higher than our result. The method used by Hernandez et al. (2007) makes several highly questionable assumptions, and thus we do not consider their result reliable. For example, Hernandez et al. (2007) assume a constant galaxy mass to dark matter mass ratio of $F = 0.04$, which corresponds to a galaxy formation efficiency of $\epsilon_{\text{GF}} \simeq 0.25$. Comparison with Fig. 2 shows that while this is a good assumption for a $2 \times 10^{12} M_{\odot}$ halo, it significantly over-estimates the galaxy formation efficiency, and hence spin parameters, of lower mass galaxies. Since Hernandez et al. (2007) use a volume limited sample, their measurement of the spin parameter is biased towards lower mass galaxies, where their assumption of $F = 0.04$ is high by a factor of $\simeq 2$. In the method used by Hernandez et al. (2007)

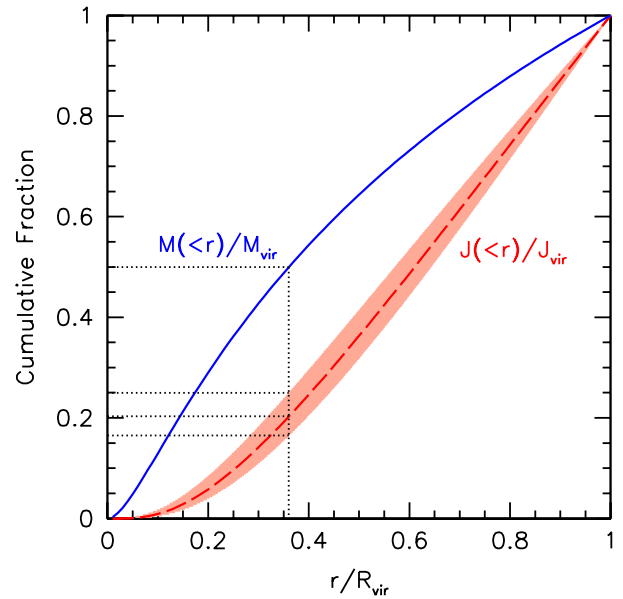


Figure 5. The cumulative, normalized fractions of mass (blue line) and angular momentum (dashed red line) for Λ CDM haloes (Navarro et al. 1997; Bullock et al. 2001). The shaded region shows the uncertainty on $J(r)/J_{\text{vir}}$ assuming $s = 1.3 \pm 0.3$ in Eq. 9. This clearly demonstrates that mass is more centrally concentrated than angular momentum. For example, the inner 50% of the mass contains just $20^{+5}_{-4}\%$ of the angular momentum (black dotted lines). Thus if the efficiency of galaxy formation is regulated by the efficiency of cooling, we would expect a strong correlation between galaxy spin parameter and galaxy formation efficiency, which is not observed.

$\lambda'_{\text{gal}} \propto F$, and thus their assumption of $F = 0.04$ accounts for at least half the discrepancy between our result and theirs.

4 COMPARISON WITH GALAXY FORMATION MODELS

4.1 Inside-Out Cooling Models

If the galaxy formation efficiency is determined by the efficiency of cooling, then we expect that \mathcal{R}_j will be higher for higher galaxy formation efficiencies. This is because in Λ CDM haloes mass is more centrally concentrated than angular momentum. This is illustrated in Fig. 5. The blue solid line shows the cumulative mass fraction, $M(<r)/M_{\text{vir}}$ as a function of radius for a NFW halo with concentration $c = 10$. The red dashed line shows the cumulative angular momentum fraction, $J(<r)/J_{\text{vir}}$, as a function of radius assuming

$$\frac{J(<r)/J_{\text{vir}}}{M(<r)/M_{\text{vir}}} = [M(<r)/M_{\text{vir}}]^s, \quad (9)$$

where $s = 1.3 \pm 0.3$ (Bullock et al. 2001). Under the assumptions that (i) the baryons initially acquire the same specific angular momentum as the dark matter, and (ii) the baryons accrete onto the central galaxy inside-out, then Eq. 9 implies $\mathcal{R}_j = \epsilon_{\text{GF}}^s$.

We now extend this simple inside-out cooling model to cosmologically evolving dark matter haloes. The red lines in

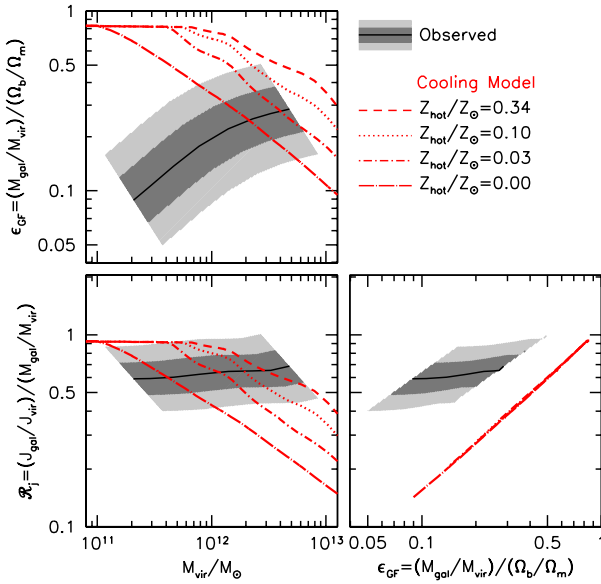


Figure 6. Correlations between halo mass, M_{vir} , galaxy formation efficiency, ϵ_{GF} , and specific angular momentum ratio, \mathcal{R}_j , for models and observations at redshift $z = 0$. The empirical relations for disc galaxies are shown as solid black lines, with the shading reflecting the one and two σ uncertainties on halo masses. Note that the galaxy formation efficiency increases with increasing halo mass, while the specific angular momentum ratio is independent of halo mass. The corresponding relations for a simple cooling model are shown with red lines, where the different line types correspond to different metallicities, as indicated. In this cooling model $\mathcal{R}_j \sim \epsilon_{\text{GF}}$ (independent of the metallicity of the hot gas), inconsistent with the empirical findings.

Fig. 6 show the relations between \mathcal{R}_j , ϵ_{GF} and M_{vir} for a scenario in which the galaxy formation efficiency is determined by the efficiency of cooling. This model is a simplified version of the galaxy formation model from Dutton & van den Bosch (2009). Briefly this model consists of NFW haloes that grow by smooth accretion of baryons and dark matter. The angular momentum of each shell of accreted gas is determined by assuming that the angular momentum distribution (AMD) of a given halo is independent of time. The AMD is specified by two parameters: the normalization (λ) and shape (α). When the baryons enter the halo they are shock heated to the virial temperature. The cooling time depends on the temperature, density and metallicity of the hot gas. We use the metallicity dependent collisional ionization equilibrium cooling functions of Sutherland & Dopita (1993). Results for four different metallicities from primordial to one third solar are shown. For low mass haloes ($M_{\text{vir}} \sim 10^{11} M_{\odot}$) cooling is very efficient, so that $\simeq 90\%$ of the baryonic mass is accreted (left-hand panels)⁵. For more massive haloes, the galaxy formation efficiency, ϵ_{GF} , depends strongly on the metallicity of the gas, with higher metallicities yielding larger values of ϵ_{GF} . Clearly, the trend that ϵ_{GF} decreases with increasing halo mass is completely opposite to the em-

⁵ It is not 100% because it takes a free fall time for the most recently accreted baryons to reach the galaxy.

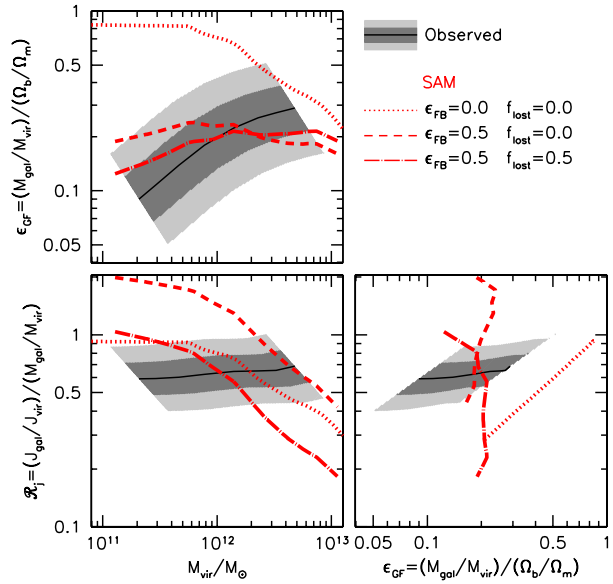


Figure 7. Same as Fig. 6, but this time we compare the empirical relations (solid black lines with shaded regions) with models that include feedback and/or angular momentum loss (red lines). All models shown adopt a hot gas metallicity of $Z_{\text{hot}} = 0.1Z_{\odot}$, but they differ in feedback efficiency, ϵ_{FB} , and the fraction of angular momentum lost by the baryons during galaxy formation, f_{lost} . The dotted line ($\epsilon_{\text{FB}} = f_{\text{lost}} = 0$) is identical to the simple cooling model from Fig. 6, and is shown for comparison. Note that none of the models is able to simultaneously match the low galaxy formation efficiencies and the constant angular momentum ratio. See text for a detailed discussion.

pirical result. As for the parameter \mathcal{R}_j , the simple cooling models predict that \mathcal{R}_j should decrease with increasing halo mass, which is a consequence of cooling being an inside-out process combined with the fact that mass is more centrally concentrated than angular momentum (cf. Fig. 5). Hence, in massive haloes where $\epsilon_{\text{GF}} \ll 1$ due to inefficient cooling, the galaxy ends up having less specific angular momentum than its dark matter halo. This strong mass dependence of \mathcal{R}_j is again inconsistent with our empirical results. Finally, the cooling models predicts an almost linear relation between \mathcal{R}_j and ϵ_{GF} , which is independent of the gas metallicity (lower right-hand panel of Fig. 6). Clearly, this linear relation is very different from its empirical equivalent, indicating that additional mechanisms for accreting and/or expelling gas are required.

4.2 Outflows and Angular Momentum Loss

We now consider two modifications to the simple cooling model: outflows and angular momentum loss. We assume that outflows, which move at the local escape velocity, are driven by energy from supernovae (SNe). The fraction of the SNe energy that goes into an outflow is specified by the free parameter ϵ_{FB} (see van den Bosch 2002; Dutton & van den Bosch 2009). Other than inefficient cooling in massive haloes, and UV heating in low mass haloes, galactic outflows are the primary mechanism for explaining the observed low galaxy formation efficiencies (e.g., Dekel &

Silk 1986; Cole et al. 1994). For simplicity, we assume that outflow gas leaves the disc and halo, and does not return. However, recent cosmological hydrodynamical simulations have shown that ejected gas may return to the galaxy (Oppenheimer et al. 2010). Some of the ejected gas may mix with the halo gas and thus re-accrete with higher specific angular momentum (Brook et al. 2012). Since this process is a re-distribution (i.e., ejected gas gains angular momentum, halo gas loses angular momentum), it does not change the specific angular momentum of the baryons. If the halo gas accretes onto the central galaxy (as is expected for low mass, $M_{\text{vir}} \lesssim 10^{12} M_{\odot}$, haloes) then there is no net change in the angular momentum of the galaxy. If the halo gas does not accrete (which is expected for high mass haloes) then the galaxy can gain angular momentum via this galactic fountain effect. Thus if we were to implement re-accretion into our model we would need higher feedback efficiencies to achieve the same galaxy formation efficiencies, but to first order there would be no change to the specific angular momentum.

We assume that during the accretion process, a fraction f_{lost} of the angular momentum of the gas is lost to the dark matter halo. The mechanism responsible for this transfer is dynamical friction. In our models we do not take into account the effects of angular momentum transfer and outflows on the structure of the dark matter halo. But we note that both of these processes will result in halo expansion, or at least a reduction of the amount of adiabatic contraction, i.e., a lower effective value of ν (e.g., Navarro et al. 1996; El-Zant et al. 2001; Mo & Mao 2004; Cole, Dehnen & Wilkinson 2011)

In Fig. 7 we show several models with different values of ϵ_{FB} and f_{lost} . In all models we assume that halo gas is enriched to one tenth solar. The dotted line shows a model with $\epsilon_{\text{FB}} = 0.0$ and $f_{\text{lost}} = 0.0$: this corresponds to the simple cooling model from Fig. 6 and is shown for comparison. The galaxy formation efficiencies are too high for all halo masses. In order to produce realistic galaxy formation efficiencies outflows are needed. A model with $\epsilon_{\text{FB}} = 0.5$ and $f_{\text{lost}} = 0.0$ (short dashed line) has $\epsilon_{\text{GF}} \sim 20\%$. In our model outflows increase \mathcal{R}_j by preferentially removing gas with low specific angular momentum. Since outflows are driven by star formation, regions that have higher star formation rates have higher mass outflow rates. Star formation is empirically more efficient at smaller galactic radii (Kennicutt 1998) as well as at higher redshifts (e.g., Noeske et al. 2007; Daddi et al. 2007; Elbaz et al. 2007). Smaller galactic radii correspond to lower specific angular momentum and discs are smaller at higher redshifts (e.g., Dutton et al. 2011a); both of these effects contribute to outflows increasing the specific angular momentum of the material that remains in the galaxy. In our energy driven outflow model the mass loading factor (\equiv outflow rate / star formation rate) is higher in lower mass galaxies, which results in \mathcal{R}_j increasing more in lower mass haloes (by up to a factor two). This increases the disagreement with the empirically inferred relation between \mathcal{R}_j and halo mass. We can lower \mathcal{R}_j by introducing angular momentum loss (i.e., setting $f_{\text{lost}} > 0$). The long dashed-dotted lines in Fig. 7 correspond to a model with $\epsilon_{\text{FB}} = 0.5$ and $f_{\text{lost}} = 0.5$. This angular momentum loss reduces \mathcal{R}_j by a factor ~ 2 at all mass scales, bringing it in reasonable agreement with the observed value for haloes with

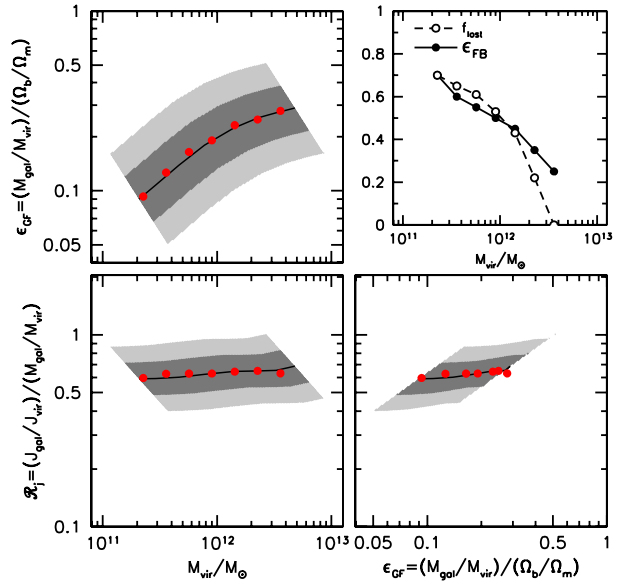


Figure 8. Same as Fig. 7, but this time we have tuned the feedback efficiency, ϵ_{FB} , and angular momentum loss, f_{lost} , of the model (red, solid dots) in order to accurately reproduce the empirical relations (solid black lines with shaded regions). The small, upper right-hand panel shows the corresponding halo mass dependence of ϵ_{FB} (solid circles) and f_{lost} (open circles): reproducing the empirical relations requires both of these parameters to decrease strongly with increasing halo mass. See text for a detailed discussion.

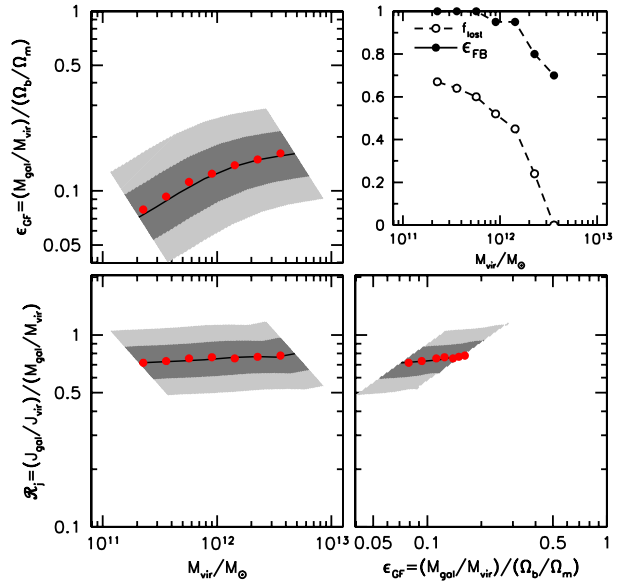


Figure 9. Same as Fig. 8, but here we have used model B (stellar mass-to-light ratios that are 0.3 dex lower and halo contraction characterized by $\nu = 0.8$) for the empirical relations. Reproducing the inferred galaxy formation efficiencies now requires even stronger feedback (i.e., larger ϵ_{FB}), while the fraction of angular momentum that is lost is similar to that for our fiducial model shown in Fig. 8.

$M_{\text{vir}} \simeq 10^{12} M_{\odot}$. However, for lower (higher) mass haloes the model overpredicts (underpredicts) the value of \mathcal{R}_j compared to the empirically inferred values. Increasing f_{lost} also modified the galaxy formation efficiency because it results in denser (smaller) discs. In low mass haloes, the galaxies are gas rich. Hence, an increase in disc density results in higher star formation rates and consequently more energy to drive outflows. This more than compensates for the higher escape velocities, resulting in lower values of ϵ_{GF} . In massive haloes, on the other hand, the galaxies are gas poor, so that an increase of the density of the disc only results in an increase of the escape velocity. This reduces the amount of ejected gas, and therefore increases ϵ_{GF} .

It is clear that none of the models discussed thus far can simultaneously reproduce the empirically inferred trends of ϵ_{GF} and \mathcal{R}_j with halo mass. As an illustration of what seems to be required, we now consider a model in which both ϵ_{FB} and f_{lost} depend on halo mass. The red filled symbols in Fig. 8 show a model in which ϵ_{FB} and f_{lost} have been tuned so that the model matches the empirical ϵ_{GF} and \mathcal{R}_j . The corresponding values of ϵ_{FB} and f_{lost} , as a function of virial mass, are shown in the upper right-hand panel. Lower mass haloes *require* higher ϵ_{FB} and f_{lost} . For example, this model has $(\epsilon_{\text{FB}}, f_{\text{lost}}) = (0.7, 0.7)$ for $M_{\text{vir}} \simeq 10^{11.3} M_{\odot}$, and $(\epsilon_{\text{FB}}, f_{\text{lost}}) = (0.25, 0.0)$ for $M_{\text{vir}} \simeq 10^{12.4} M_{\odot}$.

The results shown in Fig. 8 correspond to the empirical ϵ_{GF} and \mathcal{R}_j inferred under the assumptions of model A (i.e., Chabrier IMF and halo contraction characterized by $\nu = -0.5$). Fig. 9 shows the analogous results but for model B (an IMF that results in stellar mass-to-light ratios that are 0.3 dex lower than for model A and with $\nu = 0.8$). Reproducing the galaxy formation efficiencies now requires even stronger feedback, but with a similar mass dependence, whereas the fraction of angular momentum that is lost is similar to that of our fiducial model.

4.3 Disc Stability

Thus far we have assumed that disc galaxies form in typical dark matter haloes. This must be true at the low mass end, simply because disc galaxies dominate the galaxy population at low masses. However, at high masses disc galaxies are a minority, so that it is possible that they form in a biased subset of dark matter haloes. To reconcile our models with the empirical fact that \mathcal{R}_j seems to be independent of halo mass requires a bias such that massive disc galaxies form preferentially in haloes with larger spin parameters.

Such a bias is naturally achieved by invoking disc stability. Disc galaxies can only survive as such to the present day if their discs are sufficiently stable. Disc galaxies that are unstable redistribute their angular momentum via secular evolution, typically resulting in spheroid dominated galaxies (e.g., Combes et al. 1990; Norman, Sellwood & Hasan 1996; van den Bosch 1998; Mao & Mo 1998). Since more self-gravitating (denser) discs are more unstable (e.g., Efsthathiou, Lake & Negroponte 1982), and since the surface density of a disc is proportional to $\lambda_{\text{halo}}^{-2}$ (e.g., Mo, Mao & White 1998), one expects a bias against disc galaxies in haloes with the lowest spin parameter. Since the disc's surface density is also proportional to ϵ_{GF} , and empirically ϵ_{GF} increases with increasing halo mass, one expects discs in less massive haloes to be more stable than those in more

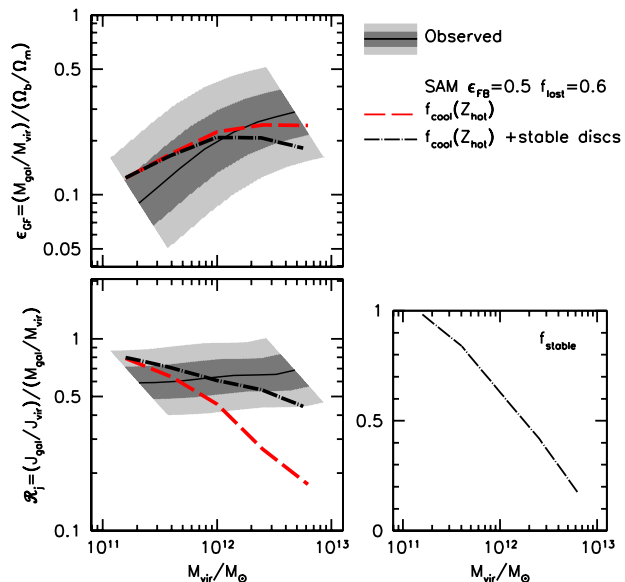


Figure 10. The impact of disc stability on the galaxy formation efficiency (ϵ_{GF} ; upper left-hand panel) and specific angular momentum ratio (\mathcal{R}_j ; lower left-hand panel). The solid line with the shaded regions indicate the empirical relations (for our fiducial model A). The dashed, red line corresponds to a simple model with $Z_{\text{hot}} = 0.1Z_{\odot}$, $\epsilon_{\text{FB}} = 0.5$ and $f_{\text{lost}} = 0.6$, which yields galaxy formation efficiencies in reasonable agreement with the data. However, it predicts that \mathcal{R}_j decreases strongly with increasing halo mass, in clear conflict with the data. The dot-dashed, black line corresponds to the same model, but now we have removed those discs that do not satisfy our disc stability criterion. This removes massive galaxies in low-spin haloes, resulting in a higher \mathcal{R}_j for mass haloes, in better agreement with the data.

massive haloes. Hence, disc stability may introduce a bias against forming *massive* disc galaxies in *low* spin parameter haloes, exactly what seems to be required.

To test the potential impact of disc stability on the relations between ϵ_{GF} , \mathcal{R}_j , and M_{vir} , we add a simple stability criterion to our models: we assume that if the disc contributes more than 84% of the mass within 2.2 disc scale lengths it will be highly unstable, and we remove these galaxies from our sample of model galaxies. We note that discs are already expected to become unstable — and hence to form bulges via secular evolution — at disc mass fractions lower than 84%. However, we choose a high stability threshold as we do not wish to remove the galaxies that remain disc dominated after secular evolution.

Fig. 10 shows the effect of disc stability on ϵ_{GF} and \mathcal{R}_j . In our fiducial model (red long-dashed lines) the fraction of gas that cools at each time step (f_{cool}) depends on the metallicity of the hot halo gas (here $Z_{\text{hot}} = 0.1Z_{\odot}$), the feedback efficiency (here $\epsilon_{\text{FB}} = 0.5$) and the fraction of angular momentum that is lost (here $f_{\text{lost}} = 0.6$). This model approximately reproduces the observed relation between galaxy formation efficiency and halo mass, but it predicts that \mathcal{R}_j decreases strongly with increasing halo mass, which is inconsistent with the empirical results. Invoking the disc stability criteria discussed above (black dot-long-dashed

lines) results in a lower fraction of stable discs in higher mass haloes (lower right panel): when computing the average \mathcal{R}_j at a given halo mass (for both models and observations), we assume that the haloes have a median spin parameter as expected from cosmological simulations (i.e., $\lambda' = 0.031$). However, since stable discs have higher median spin parameters than unstable discs, this results in stable discs having higher \mathcal{R}_j . The stable discs in our model still have an anti-correlation between \mathcal{R}_j and halo mass, but the model is now consistent with the observations at the 2σ level.

The disc stability scenario also provides a qualitative explanation for two additional observational facts: (i) the scatter in disc sizes decreases with increasing stellar mass (Shen et al. 2003), such that for the most massive discs the scatter is half that expected from the scatter in halo spin parameters (Dutton et al. 2011a); and (ii) the fraction of galaxies that are star forming disc galaxies declines with increasing galaxy and halo mass (e.g., Yang et al. 2008). Hence, we conclude that disc stability may be an important ingredient for understanding the empirical scaling relations between ϵ_{GF} , \mathcal{R}_j and halo mass.

4.4 Comparison with Hydrodynamical Simulations

The simplistic analytical models used above indicate that it is not easy to understand why the specific angular momentum ratio \mathcal{R}_j seems to be independent of halo mass, whereas the galaxy formation efficiency increases strongly with halo mass. In fact, reproducing the empirical scaling relations between ϵ_{GF} , \mathcal{R}_j and halo mass seems to require a feedback efficiency that declines with increasing halo mass.

An important downside of our simplistic models is that they do not properly account for the hydrodynamics of outflows from galaxies embedded in a large scale environment from which the galaxy is also accreting matter. This requires cosmological, hydrodynamical simulations, which arguably are the best tool available to model the complex, hierarchical nature of galaxy formation. Recently, Sales et al. (2009) have presented a suite of high resolution, hydrodynamical simulations of the formation of galaxies in a Λ CDM concordance cosmology, with a wide range of feedback recipes. Their resulting galaxies (at $z = 2$) have properties that are well fit by

$$\mathcal{R}_j = 9.71 m_{\text{gal}} [1 - \exp(-1/9.71 m_{\text{gal}})]. \quad (10)$$

independent of the feedback recipe! Here $m_{\text{gal}} = M_{\text{gal}}/M_{\text{vir}} = \epsilon_{\text{GF}} (\Omega_{\text{b}}/\Omega_{\text{m}})$ is the galaxy mass fraction. As a specific example, for a galaxy mass fraction of $m_{\text{gal}} = 0.033$ (i.e. 20% of the cosmic baryon fraction) the specific angular momentum ratio is predicted to be $\mathcal{R}_j = 0.31$. This scaling is given by the black dashed line in Fig. 11. Interestingly, the relation from Sales et al. (2009) is very similar to the results from our simple cooling model (red lines). This suggests that feedback in their simulations largely preserves the rank order in binding energy of the baryons, such that the relation between ϵ_{GF} and \mathcal{R}_j of the resulting galaxies is predominantly set by the relative radial profiles of mass and angular momentum shown in Fig. 5. It is unclear at present why the simulations seem to preserve the rank order of binding energy, but it may have to do with the fact that outflows are

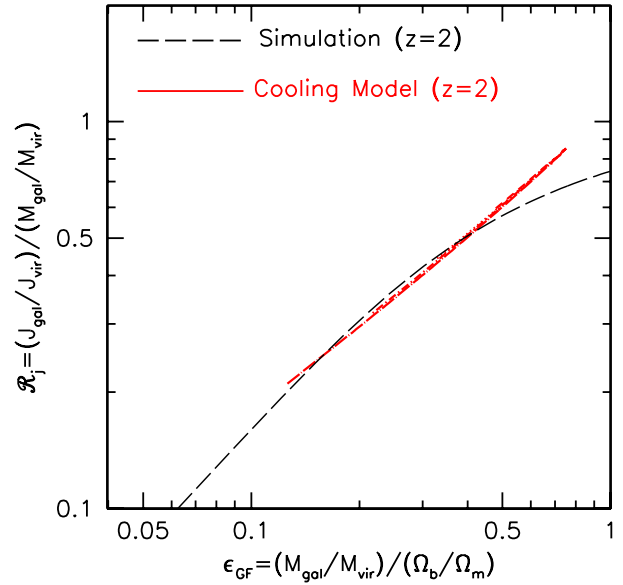


Figure 11. Correlation between specific angular momentum ratio, \mathcal{R}_j , and galaxy formation efficiency, ϵ_{GF} . The red lines show the relations from our simple inside-out cooling model with different gas metallicities (see Fig. 6). The black, dashed line shows the relation from Sales et al. (2009), obtained for simulated galaxies at $z \sim 2$ in a cosmological hydrodynamical simulation. Note that these simulated galaxies follow exactly the relation between \mathcal{R}_j and ϵ_{GF} expected for a simple cooling model, despite the fact that the simulations include supernova feedback. See text for a detailed discussion.

inhibited from travelling far from their source due to pressure confinement of the surrounding gas, an effect that is not accounted for in our simplistic, analytical models. Irrespective of what causes the relation between \mathcal{R}_j and ϵ_{GF} in the simulations, it is clear that Eq. 10 is inconsistent with the empirical relation. We caution, though, that the simulations were only run to redshift $z = 2$, whereas our empirical results correspond to $z \simeq 0$. In addition, our empirical results are for star-forming disc-dominated galaxies, whereas the results from the simulations are for all types of galaxies. It remains to be seen whether simulations of disc formation that are run to $z = 0$ yield a relation between \mathcal{R}_j and ϵ_{GF} in better agreement with the data.

5 SUMMARY

We have combined measurements of halo virial masses from weak lensing and satellite kinematics with the Tully-Fisher and size-mass relations of disc galaxies (i.e., star-forming and disc-dominated) to infer the average spin parameter of disc galaxies as a function of their halo mass. Using toy models for disc galaxy formation we have discussed implications of these results for cooling, outflows and angular momentum loss. We summarize our results as follows:

- The average galaxy spin parameters of disc galaxies are consistent with being independent of halo mass for the range of halo masses probed here: $11.3 \leq \log_{10}(M_{\text{vir}}/M_{\odot}) \leq 12.7$.

- The primary uncertainty in measuring the spin parameters of galaxies is the determination of halo masses. Realistic uncertainties of 0.25 dex (2σ), result in uncertainties in galaxy spin parameters of a factor of 1.5. A secondary uncertainty is the stellar IMF. Since gas discs have higher specific angular momentum than stellar discs, lower stellar mass normalizations will result in higher spin parameters. For example, stellar masses lower by 0.3 dex result in spin parameters higher by 0.12 dex.

- The average spin parameter of galaxies, $\langle \lambda_{\text{gal}} \rangle = 0.019_{-0.003}^{+0.004}$ (1σ), is smaller than that of their host dark matter haloes, $\langle \lambda_{\text{halo}} \rangle = 0.031 \pm 0.001$ (Macciò et al. 2007, 2008; Bett et al. 2007). The inferred spin parameters of disc galaxies reveal no dependence on halo mass, so that the specific angular momentum ratio $\mathcal{R}_j \simeq 0.6$, independent of halo mass. The galaxy formation efficiency parameter, ϵ_{GF} , however, reveals a strong mass dependence, increasing from $\sim 10\%$ for $M_{\text{vir}} = 10^{11.5} M_{\odot}$ to $\sim 30\%$ for $M_{\text{vir}} = 10^{12.5} M_{\odot}$ for our fiducial model.

- Since mass is more centrally concentrated than angular momentum in Λ CDM haloes a simple inside-out accretion model results in a strong correlation between galaxy spin parameter and galaxy formation efficiency, contrary to observations. This provides further support for the already popular notion that the low galaxy formation efficiencies in haloes of mass $M_{\text{vir}} \lesssim 10^{11.7} M_{\odot}$ are determined primarily by feedback processes, and not by an inefficiency of cooling.

- The empirically inferred relations between galaxy formation efficiency, ϵ_{GF} , angular momentum ratio, \mathcal{R}_j , and halo mass seem to indicate that galaxy formation involves galactic outflows, or other mechanisms that can regulate the galaxy formation efficiency (e.g., supernova feedback, AGN feedback, reionization, pre-heating), as well as mechanisms that cause a substantial transfer of angular momentum from the baryons to the dark matter (e.g., dynamical friction). Although the need for feedback mechanisms to regulate the efficiency of galaxy formation has long been recognized, the observed scaling relations for disc galaxies seem to require that the often adopted supernovae feedback efficiency parameter, ϵ_{FB} , decreases with halo mass. In addition, the angular momentum content of observed disc galaxies also require that angular momentum loss is more important for disc formation in less massive haloes. It remains to be seen whether realistic models for galaxy formation can achieve effective values for ϵ_{FB} and f_{lost} that reveal such a dependence on halo mass.

What could be the cause for the *effective* values for ϵ_{FB} and f_{lost} to decrease with increasing halo mass? One possibility is that this mass dependence is a manifestation of the transition from cold-mode accretion at $M_{\text{vir}} \lesssim 10^{11.7} M_{\odot}$ to hot-mode accretion for haloes with $M_{\text{vir}} \gtrsim 10^{11.7} M_{\odot}$ (e.g., Birnboim & Dekel 2003; Keres et al. 2005, 2009; Brooks et al. 2009). In the cold mode regime, outflows are unhindered by hot-gas atmospheres, which may result in higher effective feedback efficiencies. If, as envisioned in our models, the outflows preferentially remove low angular momentum material, the same outflows which reduce the galaxy formation efficiency are expected to increase the specific angular momentum ratio, \mathcal{R}_j . Hence, in order to reproduce the inferred $\mathcal{R}_j \simeq 0.6$, the baryons that end up in the disc need to lose a significant fraction ($\sim 60\%$) of their angular momen-

tum during the galaxy formation process. If the cold accretion is sufficiently clumpy, this may come about because of dynamical friction.

In the hot mode accretion regime, outflows are expected to be less efficient, since they have to do work against their hot gaseous atmospheres. In this regime, one expects that the baryon fraction and angular momentum of the resulting disc galaxies are largely determined by the inside-out cooling of the hot gas, resulting in \mathcal{R}_j decreasing strongly with increasing halo mass. This, however, is inconsistent with the empirical result that \mathcal{R}_j appears to be independent of halo mass. We have argued that disc stability may play an important role here, effectively removing systems with low halo spin parameter from the sample of disc galaxies (because they produce unstable discs), thereby increasing the average \mathcal{R}_j of massive disc galaxies. Another important process may be that at high redshifts ($z \gtrsim 2$), massive haloes in the hot-mode accretion regime can still accrete a significant amount of material via cold streams that penetrate the hot halo (e.g., Dekel et al. 2009). Depending on the ‘impact parameters’ of such streams, the cold material thus deposited to the central galaxy may have specific angular momentum that is relatively high, boosting the value of \mathcal{R}_j with respect to that expected in a simple cooling model.

Although plausible, we caution that the above discussion regarding the potential impact of the cold-mode to hot-mode accretion regime is highly speculative. In fact, the high resolution, hydrodynamical simulations of Sales et al. (2009), which in principle should naturally account for the cold mode *vs.* hot mode effects mentioned above, did not yield (disc) galaxies with the correct relation between ϵ_{GF} and \mathcal{R}_j . Amazingly enough, their simulated galaxies revealed a tight, linear correlation between ϵ_{GF} and \mathcal{R}_j in perfect agreement with our predictions for a simple cooling model, *despite the fact that their simulations included star formation and feedback (using several different implementations)*. If taken at face value, these simulations seem to suggest that feedback has little to no effect on the ϵ_{GF} *vs.* \mathcal{R}_j relation; although it reduces ϵ_{GF} , it causes a similar suppression of \mathcal{R}_j . In addition, the Sales et al. simulations (which were only run to $z = 2$) seem to indicate that cold mode accretion, which should have been the dominant mode of accretion for the galaxies in their simulations, does not have the effect envisioned above. More detailed hydrodynamical simulations of galaxy formation (run all the way to $z = 0$) are needed to investigate these issues in more detail. In particular, we currently lack a proper understanding of how cold mode accretion and cold streams contribute to the build-up of mass and, in particular, angular momentum of disc galaxies.

ACKNOWLEDGMENTS

We thank Julio Navarro for useful discussions. AAD acknowledges financial support from the Canadian Institute for Theoretical Astrophysics (CITA) National Fellows Program.

REFERENCES

- Abadi, M. G., Navarro, J. F., Feudal, M., Babul, A., & Steinmetz, M. 2010, *MNRAS*, 407, 435
- Barden, M., et al. 2005, *ApJ*, 635, 959
- Berta, Z. K., Jimenez, R., Heavens, A. F., & Panter, B. 2008, *MNRAS*, 391, 197
- Bett, P., Eke, V., Frenk, C. S., Jenkins, A., Helly, J., & Navarro, J. 2007, *MNRAS*, 376, 215
- Birnboim, Y., & Dekel, A. 2003, *MNRAS*, 345, 349
- Blumenthal, G. R., Faber, S. M., Flores, R., & Primack, J. R., 1986, *ApJ*, 301, 27
- Brook, C. B., et al. 2011, *MNRAS*, 415, 1051
- Brook, C. B., Stinson, G., Gibson, B. K., et al. 2012, *MNRAS*, 419, 771
- Brooks, A. M., Governato, F., Quinn, T., Brook, C. B., & Wadsley, J. 2009, *ApJ*, 694, 396
- Bullock, J. S., Dekel, A., Kolatt, T. S., Kravtsov, A. V., Klypin, A. A., Porciani, C., & Primack, J. R. 2001, *ApJ*, 555, 240
- Burkert, A. 1995, *ApJL*, 447, L25
- Cacciato, M., van den Bosch, F. C., More, S., Li, R., Mo, H. J., & Yang, X. 2009, *MNRAS*, 394, 929
- Chabrier, G. 2003, *PASP*, 115, 763
- Cole, S., Aragon-Salamanca, A., Frenk, C. S., Navarro, J. F., & Zepf, S. E. 1994, *MNRAS*, 271, 781
- Cole, S., Lacey, C. G., Baugh, C. M., & Frenk, C. S. 2000, *MNRAS*, 319, 168
- Cole, D. R., Dehnen, W., & Wilkinson, M. I. 2011, *MNRAS*, 416, 1118
- Combes, F., Debbasch, F., Friedli, D., & Pfenniger, D. 1990, *A&A*, 233, 82
- Conroy, C., Wechsler, R. H., & Kravtsov, A. V. 2006, *ApJ*, 647, 201
- Daddi, E., et al. 2007, *ApJ*, 670, 156
- Dalcanton, J. J., Spergel, D. N., & Summers, F. J. 1997, *ApJ*, 482, 659
- de Jong, R. S., & Lacey, C. 2000, *ApJ*, 545, 781
- Dekel, A., & Silk, J. 1986, *ApJ*, 303, 39
- Dekel, A., et al. 2009, *Nature*, 457, 451
- D'Onghia, E., & Burkert, A. 2004, *ApJL*, 612, L13
- Dutton, A. A., van den Bosch, F. C., Dekel, A., & Courteau, S. 2007, *ApJ*, 654, 27
- Dutton, A. A. 2009, *MNRAS*, 396, 121
- Dutton, A. A., & van den Bosch, F. C. 2009, *MNRAS*, 396, 141
- Dutton, A. A., van den Bosch, F. C., & Dekel, A. 2010a, *MNRAS*, 405, 1690
- Dutton, A. A., Conroy, C., van den Bosch, F. C., Prada, F., & More, S. 2010b, *MNRAS*, 407, 2
- Dutton, A. A., et al. 2011a, *MNRAS*, 410, 1660
- Dutton, A. A., Conroy, C., van den Bosch, F. C., et al. 2011b, *MNRAS*, 416, 322
- Efstathiou, G., Lake, G., & Negroponte, J. 1982, *MNRAS*, 19, 1069
- Eke, V., Efstathiou, G., & Wright, L. 2000, *MNRAS*, 315, L18
- Elbaz, D., et al. 2007, *A&A*, 468, 33
- El-Zant, A., Shlosman, I., & Hoffman, Y. 2001, *ApJ*, 560, 636
- Fall, S. M., & Efstathiou, G. 1980, *MNRAS*, 193, 189
- Firmani, C., & Avila-Reese, V. 2000, *MNRAS*, 315, 457
- Firmani, C., & Avila-Reese, V. 2009, *MNRAS*, 396, 1675
- Gnedin, O. Y., Kravtsov, A. V., Klypin, A. A., & Nagai, D. 2004, *ApJ*, 616, 16
- Governato, F., et al. 2004, *ApJ*, 607, 688
- Governato, F., et al. 2010, *Nature*, 463, 203
- Hernandez, X., & Cervantes-Sodi, B. 2006, *MNRAS*, 368, 351
- Hernandez, X., Park, C., Cervantes-Sodi, B., & Choi, Y.-Y. 2007, *MNRAS*, 375, 163
- Hernquist, L., 1990, *ApJ*, 356, 359
- Hopkins, P. F., Cox, T. J., Younger, J. D., & Hernquist, L. 2009, *ApJ*, 691, 1168
- Kauffmann, G. 1996, *MNRAS*, 281, 475
- Kaufmann, T., Mayer, L., Wadsley, J., Stadel, J., & Moore, B. 2007, *MNRAS*, 375, 53
- Kennicutt, R. C. 1998, *ApJ*, 498, 541
- Kereš, D., Katz, N., Weinberg, D. H., & Davé, R. 2005, *MNRAS*, 363, 2
- Kereš, D., Katz, N., Fardal, M., Davé, R., & Weinberg, D. H. 2009, *MNRAS*, 395, 160
- Lemson, G., & Kauffmann, G. 1999, *MNRAS*, 302, 111
- Macciò, A. V., Dutton, A. A., van den Bosch, F. C., Moore, B., Potter, D., & Stadel, J. 2007, *MNRAS*, 378, 55
- Macciò, A. V., Dutton, A. A., & van den Bosch, F. C. 2008, *MNRAS*, 391, 1940
- Maller, A. H., & Dekel, A. 2002, *MNRAS*, 335, 487
- Mandelbaum, R., Seljak, U., Kauffmann, G., Hirata, C. M., & Brinkmann, J. 2006, *MNRAS*, 368, 715
- Mao, S., & Mo, H. J. 1998, preprint (arXiv:astro-ph/9805094)
- Mo, H. J., Mao, S., & White, S. D. M. 1998, *MNRAS*, 295, 319
- Mo, H. J., & Mao, S. 2004, *MNRAS*, 353, 829
- Mo, H. J., van den Bosch, F. C., & White, S. D. M. 2010, *Galaxy Formation and Evolution*, Cambridge University Press
- More, S., van den Bosch, F. C., Cacciato, M., Mo, H. J., Yang, X., & Li, R. 2009, *MNRAS*, 392, 801
- Muñoz-Cuartas, J. C., Macciò, A. V., Gottlöber, S., & Dutton, A. A. 2011, *MNRAS*, 411, 584
- Navarro, J. F., & Benz, W. 1991, *ApJ*, 380, 320
- Navarro, J. F., & White, S. D. M. 1994, *MNRAS*, 267, 401
- Navarro, J. F., Eke, V. R., & Frenk, C. S. 1996, *MNRAS*, 283, L72
- Navarro, J. F., Frenk, C. S., & White, S. D. M. 1997, *ApJ*, 490, 493 (NFW)
- Navarro, J. F., & Steinmetz, M. 1997, *ApJ*, 478, 13
- Navarro, J. F., & Steinmetz, M. 2000, *ApJ*, 538, 477
- Noeske, K. G., et al. 2007, *ApJL*, 660, L43
- Norman, C. A., Sellwood, J. A., & Hasan, H. 1996, *ApJ*, 462, 114
- Oppenheimer, B. D., Davé, R., Kereš, D., Fardal, M., Katz, N., Kollmeier, J. A., & Weinberg, D. H. 2010, *MNRAS*, 406, 2325
- Peebles 1969, *ApJ*, 155, 393
- Piontek, F. & Steinmetz, M. 2009, preprint (astro-ph/09094156)
- Piontek, F., & Steinmetz, M. 2011, *MNRAS*, 410, 2625
- Reid, M. J., Readhead, A. C. S., Vermeulen, R. C., & Treuhaft, R. N. 1999, *ApJ*, 524, 816
- Sales, L. V., Navarro, J. F., Schaye, J., Dalla Vecchia, C., Springel, V., Haas, M. R., & Helmi, A. 2009, *MNRAS*,

- 399, L64
- Sales, L. V., Navarro, J. F., Schaye, J., Vecchia, C. D., Springel, V., & Booth, C. M. 2010, *MNRAS*, 409, 1541
- Sharma, S., & Steinmetz, M. 2005, *ApJ*, 628, 21
- Shen, S., Mo, H. J., White, S. D. M., Blanton, M. R., Kauffmann, G., Voges, W., Brinkmann, J., & Csabai, I. 2003, *MNRAS*, 343, 978
- Smith, M. C., Ruchti, G. R., Helmi, A., et al. 2007, *MNRAS*, 379, 755
- Somerville, R. S., & Primack, J. R. 1999, *MNRAS*, 310, 1087
- Somerville, R. S., et al. 2008, *ApJ*, 672, 776
- Sommer-Larsen, J., Gelato, S., & Vedel, H. 1999, *ApJ*, 519, 501
- Springel, V., & Hernquist, L. 2005, *ApJL*, 622, L9
- Steinmetz, M., & Navarro, J. F. 1999, *ApJ*, 513, 555
- Sutherland, R. S., & Dopita, M. A. 1993, *ApJS*, 88, 253
- Tinker, J. L., Weinberg, D. H., Zheng, Z., & Zehavi, I. 2005, *ApJ*, 631, 41
- Tonini, C., Lapi, A., Shankar, F., & Salucci, P. 2006, *ApJL*, 638, L13
- Trujillo, I., et al. 2006, *ApJ*, 650, 18
- Tully, R. B., & Fisher, J. R. 1977, *A&A*, 54, 661
- van den Bosch, F. C. 1998, *ApJ*, 507, 601
- van den Bosch, F. C. 2000, *ApJ*, 530, 177
- van den Bosch, F. C., Burkert, A., & Swaters, R. A. 2001, *MNRAS*, 326, 1205
- van den Bosch, F. C. 2002, *MNRAS*, 332, 456
- van den Bosch, F. C., Abel, T., Croft, R.A.C., Hernquist, L., & White, S.D.M., 2002, *ApJ*, 576, 21
- Weil, M. L., Eke, V. R., & Efstathiou, G. 1998, *MNRAS*, 300, 773
- Widrow, L. M., Pym, B., & Dubinski, J. 2008, *ApJ*, 679, 1239
- Williams, R. J., Quadri, R. F., Franx, M., van Dokkum, P., Toft, S., Kriek, M., & Labbé, I. 2010, *ApJ*, 713, 738
- Xue, X. X., Rix, H. W., Zhao, G., et al. 2008, *ApJ*, 684, 1143
- Yang, X., Mo, H. J., & van den Bosch, F. C. 2003, *MNRAS*, 339, 1057
- Yang, X., Mo, H. J., & van den Bosch, F. C. 2008, *ApJ*, 676, 248